HHS Public Access

Author manuscript

Placenta. Author manuscript; available in PMC 2016 April 01.

Published in final edited form as:

Placenta. 2015 April ; 36(4): 389–396. doi:10.1016/j.placenta.2015.01.012.

Loss of inherited genomic imprints in mice leads to severe disruption in placental lipid metabolism

K. P. Himes[a], **A. Young**[b], **E. Koppes**[b], **D. Stolz**[c], **Y. Barak**[a,b], **Y. Sadovsky**[a,b], and **J.R. Chaillet**[a]

A. Young: alexandria.n.young@gmail.com; E. Koppes: koppesea@mwri.magee.edu; D. Stolz: dstolz@pitt.edu; Y. Barak: baraky@mwri.magee.edu; Y. Sadovsky: ysadovsky@mwri.magee.edu; J.R. Chaillet: chailletjr@mwri.magee.edu

[a]Magee-Womens Research Institute, Department of Obstetrics, Gynecology and Reproductive Sciences, University of Pittsburgh School of Medicine, 204 Craft Avenue, Pittsburgh, PA 15213 USA

[b]Magee-Womens Research Institute, Department of Microbiology and Molecular Genetics, University of Pittsburgh School of Medicine, 204 Craft Avenue, Pittsburgh, PA 15213 USA

[c]Department of Cell Biology, Center for Biologic Imaging, University of Pittsburgh School of Medicine, Pittsburgh, PA 15213 USA

Abstract

Introduction—Monoallelic expression of imprinted genes is necessary for placental development and normal fetal growth. Differentially methylated domains (DMDs) largely determine the parental-specific monoallelic expression of imprinted genes. Maternally derived DNA (cytosine-5-) -methyltransferase 1o (DNMT1o) maintains DMDs during the eight-cell stage of development. DNMT1o-deficient mouse placentas have a generalized disruption of genomic imprints. Previous studies have demonstrated that DNMT1o deficiency alters placental morphology and broadens the embryonic weight distribution in late gestation. Lipids are critical for fetal growth. Thus, we assessed the impact of disrupted imprinting on placental lipids.

Methods—Lipids were quantified from DNMT1o-deficient mouse placentas and embryos at E17.5 using a modified Folch method. Expression of select genes critical for lipid metabolism was quantified with RT-qPCR. Mitochondrial morphology was assessed by TEM and mitochondrial aconitase and cytoplasmic citrate concentrations quantified. DMD methylation was determined by EpiTYPER.

Results—We found that DNMT1o deficiency is associated with increased placental triacylglycerol levels. Neither fetal triacylglycerol concentrations nor expression of select genes

Corresponding author: Katherine Himes, MD, MSc, Magee-Womens Research Institute, Department of Obstetrics, Gynecology and Reproductive Sciences, University of Pittsburgh School of Medicine, 204 Craft Avenue, Pittsburgh, PA 15213, USA, Phone: 001 (412) 641-1805, Fax: 001 (412) 641-1133, himekp@upmc.edu.

that mediate placental lipid transport were different from wild type. Placental triacylglycerol accumulation was associated with impaired beta-oxidation and abnormal citrate metabolism with decreased mitochondrial aconitase activity and increased cytoplasmic citrate concentrations. Loss of methylation at the MEST DMD was strongly associated with placental triacylglycerol accumulation.

Discussion—A generalized disruption of genomic imprints leads to triacylglycerol accumulation and abnormal mitochondrial function. This could stem directly from a loss of methylation at a given DMD, such as MEST, or represent a consequence of abnormal placental development.

Keywords

Genomic imprinting; Lipids; Triacylglycerols; Mitochondria; DNMT1

Introduction

Genomic imprinting is a molecular process that distinguishes parental alleles such that one allele is transcriptionally active. The majority of imprinted genes are organized in clusters containing a variable number of imprinted genes. The imprinted expression of genes is determined by differentially methylated domains (DMDs) within imprinting control regions (1).

Proper inheritance of methylation imprints is essential for development, with isoforms of the DNA (cytosine-5-) methyltransrease1 (DNMT1) protein playing a central role. The somatic isoform, DNMT1s, maintains methylation at most preimplantation stages (2, 3). The enzyme DNMT1o maintains DMD methylation in the 8-cell embryo. DNMT1o is synthesized in the maternal oocyte (4-6). Post-implantation embryos and placentas derived from DNMT1o-deficient oocytes lose methylation on ∼50% of the normally methylated alleles of their DMDs (2). Maintenance of maternal DNA methylation is unaffected by DNMT1o deficiency.

Imprinted genes are highly expressed in the placenta and regulate fetal growth (7). Previous investigations have demonstrated that imprinted genes modulate nutrient delivery to the fetus (8, 9) (10). While these and other data provide a connection between imprinted genes and placental carbohydrate storage and dissemination, little is known about the relationship between imprinting and placental lipids.

Transplacental supply of lipids is critical for fetal growth, particularly late in gestation (11, 12). Free fatty acids and cholesterol are the predominant lipids transferred from the maternal circulation to the fetus (13, 14). The placenta is also capable of *de novo* lipid synthesis. The mechanisms that determine delivery of lipids to the fetus remain incompletely understood. Given the important role imprinted genes play in regulating fetal growth and nutrient delivery, we hypothesized that genomic imprinting is a plausible regulator of placental lipids. The loss of DNMT1o provides an opportunity to analyze the collective contribution of genomic imprinting to these processes by stochastic elimination of DMD methylation at many sites.

We have previously reported that DNMT1o deficiency results in abnormal placental morphology and altered embryonic growth. Pathway analysis of microarray gene expression data from E17.5 DNMT1o-deficient placentas identified genes regulating the accumulation of lipids as dysregulated. Here we extended our research to investigate whether DNMT1o deficiency altered placental lipid accumulation at E17.5. (15).

Materials and Methods

Animals

The mutant *Dnmt1*$^{\Delta 1o}$ allele was maintained in the wild type 129/SvTac strain background and homozygous *Dnmt1* $^{\Delta 1o/\Delta 1o}$ (maternal genotype), heterozygous *Dnmt1* $^{\Delta 1o/+}$ (paternal genotype), and wt mice compared in this background. Mice were genotyped and sexed as described (6) (15). Primers are included in Supplemental Table 1. Experiments were performed in compliance with guidelines established by the Institutional Animal Care and Use Committee of the University of Pittsburgh. The average DNMT1o litter size at E17.5 was 2.6 versus 6.6 in WT and 53.8% of DNMT1o-deficient conceptuses were male. Consistent with our previous work, viable DNMT1o- deficient embryos and placentas were larger than WT (median embryonic weight 1002 mg (IQR: 911mg, 1067 mg) vs. 922mg (IQR: 820mg, 988mg) and median placental weight 120 mg (IQR: 112mg, 130mg) vs. 80 mg (IQR: 75mg, 90mg) (15).

Placenta dissection

Copulation was determined by the presence of a vaginal plug, and embryonic day zero (E0) was assumed to be midnight. Placentas for DNA and RNA extraction were dissected from the embryo, decidua, and yolk sac tissue and kept individually in RNA*later* (Sigma-Aldrich, St. Louis, MO). To assess for contamination from maternal decidua, we quantified the absolute expression of decidua-specific genes in WT and DNMT1o-deficient placenta by microarray and found expression to be low. For placental lipid staining, the decidua was preserved.

Determinations of DMD methylation

Genomic DNA was extracted from E17.5 placentas using AllPrep DNA/RNA Mini Kit (Qiagen, Valencia, CA). Genomic DNA methylation patterns of 11 DMDs in E17.5 placentas were determined by EpiTYPER application (Sequenom, San Diego, CA) as previously described (16). While the exact number of germ line DMDs is unknown, estimates range from 13-20. The 11 DMDs we examined contain genes highly expressed in the placenta (7, 17).

Oil red O staining

Placentas were collected in PBS, bisected and half fixed overnight at 4 °C in 4% paraformaldehyde (PFA) in PBS. PFA-fixed samples were immersed in 10%, then 20%, sucrose in PBS, followed by optimal cutting temperature (OCT) compound (Tissue-Tek, Sakura, Torrance, CA) embedding. Cryosections (10μm) were stained with oil red O (ORO) and counterstained with hematoxylin.

Quantitative measurement of gene expression

RNA was extracted using the AllPrep DNA/RNA Mini Kit (Qiagen). Contaminating DNA was removed by DNase. Complementary DNA was prepared from 1 μg RNA using the High-Capacity cDNA Reverse Transcription Kit (Applied Biosystems, Foster City, CA). RT-qPCR was performed in triplicate, using SYBR Green PCR Master Mix and the 7900HT Fast Real-Time PCR System (both from Applied Biosystems). Dissociation curves were run to ensure amplification of a single product. A template control was run for each primer set and samples analyzed using the DDCt method (18). Ribosomal protein L32 was used as the internal control.

Metabolomic analysis

Global biochemical profiles were determined by Metabolon, Inc., from 20 DNMT1o-deficient (10 male and 10 female) and ten WT placentas (5 male and 5 female) as previously described (ref). Samples were extracted and split into equal parts for analysis on the GC/MS and LC/MS/MS platforms (19, 20). Following log transformation and imputation of missing values with the minimum observed values for each compound, ANOVA contrasts were used to identify chemicals that differed significantly between the two experimental groups. Results were adjusted for multiple comparisons using an estimate of the false discovery rate (q value) with a $q < 0.02$.

Triacylglycerol and cholesterol assays

After killing, maternal whole blood was collected by intracardiac aspiration and fetal blood collected from the neck veins. Samples were stored at 4°C overnight, centrifuged at 900 g for 10 min. and serum used for analysis. For triacylglycerol assays from tissue, lipid was extracted from homogenized liver or placenta by the Folch method (21). A chloroform/methanol mix based on the Folch method was used to extract triacylglycerols from the serum. Triacylglycerol concentration was determined using a triacylglycerol quantification kit (BioVision, San Francisco, CA) and detected using a VersaMax microplate reader (Molecular Devices, Sunnyvale, CA). Cholesterol concentrations were quantified using a cholesterol quantification kit (BioVision, San Francsico CA). Tissues were homogenized in glass tubes with chloroform, isopropanol and NP-40 using Teflon pestle (Thomas Scientific). Concentrations were determined using a VersaMax microplate reader (Molecular Devices, Sunnyvale, CA). Assays were performed in duplicate.

Transmission electron microscopy

Mouse placentas were immersion-fixed with 2.5% glutaraldehyde plus 2% paraformaldehyde in PBS at 4 °C and then processed for electron microscopy as previously described (22). Ultrathin (60-nm) sections were imaged using a JEOL JEM 1011 transmission electron microscope (Peabody, MA) at 80 kV fitted with a side mount AMT 2k digital camera (Advanced Microscopy Techniques, Danvers, MA).

Cellular fractionation

Cellular fractionation was performed using a modification of a previously published protocol (23). To remove any contaminating Percoll, the mitochondrial fraction was centrifuged at 100,000 g for 90 min at 4C.

Immunoblotting

Cytoplasmic fractions were boiled in reducing buffer (40mM Tris-HCL pH 6.8, 2mM 2-mercaptoethanol, 2% (w/v) SDS, 4% (v/v) glycerol, and bromophenol blue). Mitochondrial fractions were treated with equal amounts 5× reducing buffer and 8 M urea (BP-169-500; Fisher). Samples were subjected to Tris-glycine SDS-PAGE in a 5% (w/v) polyacrylamide stacking gel with a 15% (w/v) polyacrylamide separating gel. Proteins were transferred to a 0.2 μm Immun-Blot PVDF Membrane (1620177; Bio-Rad, Hercules, CA) by wet transfer. The membrane was blocked with 5.0% BSA in TBS containing 0.1% Tween-20 for 2 h and incubated with primary antibodies (mouse cytochrome c antibody, sc-13561, 1:1000; Santa Cruz Biotechnology, Santa Cruz, CA or mouse GAPDH antibody, ab-9484, 1:40,000; Abcam, Cambridge, MA) overnight at 4 °C. Primary antibodies were revealed with secondary antibodies (goat anti-mouse IgG-HRP, sc-2005, 1:20-30,000; Santa Cruz). Signals were detected using Amersham ECL Prime Western Blotting Detection Reagent (GE Healthcare, Waukesha, WI) and visualized with CL-XPosure Film (Pierce).

Mitochondrial aconitase activity and cytoplasmic citrate concentration

Aconitase activity was determined in mitochondrial fractions according to the manufacturer's instructions, using the Aconitase Activity Kit from BioVision. Aconitase activity was expressed as the amount of citrate metabolized to isocitrate in 1 min. Cytoplasmic citrate concentration was determined with the Citrate Assay Kit (BioVision), according to the manufacturer's instructions. Results were normalized to protein content.

Statistical analysis

Kruskal-Wallis was used for nonparametric analysis. Normality was assessed by sktest. Outcome variables were log transformed to a normal distribution and linear regression used to assess the association of embryonic weight and placental triacylglycerol concentration and placental triacylglycerol concentration and DMD methylation. Analyses were done using Stata13 (StataCorp, College Station, TX).

Results

Generalized disruption of genomic imprints leads to increased neutral lipids in the placenta

We found that in contrast to WT placentas that exhibited minimal ORO staining, DNMT1o-deficient placentas had a range of ORO staining patterns, with many demonstrating significant lipid accumulation (Fig. 1, panels B). Other placentas (panel C,D) exhibited less, but still in excess of WT placentas. To confirm our ORO findings and characterize the structure of the DNTM1o-deficient labyrinth zone further, we used transmission electron microscopy (TEM). As seen in Figure 1E, WT placenta have a trilaminar structure

composed of a single layer of sinusoidal trophoblast giant cells (stgc) and 2 layers of syncytiotrophoblasts (I and II). The TEM findings of DNMT1o-deficient labyrinth zones varied widely. Figure 1, Panels F and G illustrate the extremes, with Panel 1F resembling WT and Panel 1G demonstrating complete disruption of the trilaminar structure. TEM also confirmed the ORO staining with massive lipid droplets seen in some placentas (Fig.1G). This range of findings is consistent with the mosaic phenotype previously described, that results from stochastic loss of DMD methylation at the 8 cell followed by random chromosome segregation (4, 15).

ORO stains neutral lipids, including triacylglycerols and cholesterol species. Thus, we quantitatively distinguished the accumulation of these fat classes (Fig. 1H and 1I). Our analyses demonstrated that these placentas accumulated triacylglycerols in excess of WT placentas, with DNMT1o-deficient placentas having a median concentration of 3.7nmol/mg compared to 2.1nmol/mg in WT. There was no difference in cholesterol concentrations between DNMT1o-deficient placentas and WT. We found no significant sex differences in lipid accumulation. Among DNMT1o-deficient embryos, placental triacylglycerol content and embryonic weight were inversely related (Fig. 1J).

Accumulation of triacylglycerols in the placenta is not associated with differences in triacylglycerol concentrations in the fetus

To determine whether accumulation of triacylglycerols in the placenta was associated with changes in triacylglycerol concentrations in the fetal compartment, we quantified triacylglycerols in the maternal and fetal liver and serum and characterized the expression of select transcripts associated with placental lipid trafficking. There was no difference in triacylglycerol concentration in the maternal or fetal compartments between WT and DNMT1o-deficient embryos. Additionally, there was no difference in expression of select genes responsible for placental triacylglycerol trafficking (Fig. 2C-D).

Fatty acid oxidation is disrupted in DNMT1o-deficient placentas

Placental fatty acids are largely stored as triacylglycerols within lipid droplets or oxidized for energy via beta-oxidation in mitochondria (24, 25). For beta-oxidation, long-chain fatty acids are conjugated to carnitine for transport across the inner mitochondrial membrane (Fig. 3A). Abnormal beta-oxidation of fatty acids results in lipid accumulation. We therefore assessed intermediates involved in fatty acid oxidation by profiling the metabolomic signature of DNMT1o-deficient placentas. Table 1 outlines all the lipid sub-pathways measured. Carnitine metabolism had the most disrupted biochemicals of all the lipid sub-pathways (Fig. 3B). These included acylcarnitines of all chain lengths, suggesting perturbed fatty acid oxidation. Transcription of select genes involved in fatty acid oxidation, however, was not different from WT, thus we hypothesized that abnormal fatty acid oxidation was indicative of broader mitochondrial dysfunction (Fig. 3C).

DNMT1o deficiency leads to abnormal citrate metabolism

As a first step to assess mitochondrial function, we characterized the morphology of mitochondria in the labyrinth. The mitochondria from DNMT1o-deficient placentas were swollen with a hypodense matrix and abnormal cristae (Fig. 4A). The metabolomic data

further supported our hypothesis that normal mitochondrial function was impaired in DNMT1o-deficient placentas. Citrate, a metabolite that connects the citric acid cycle in the mitochondria to fatty acid synthesis in the cytosol, was the metabolite with the second highest differential between DNMT1o and WT placentas in our global metabolomic profile (see red annotation in Fig. 4B). This suggested that conversion of citrate to isocitrate by mitochondrial aconitase was impaired. In support of this notion, reduced mitochondrial aconitase activity and increased cytoplasmic citrate levels were observed in mutant placentas (Fig. 4C,D,E). The Cytochrome C western blot confirmed that the cellular fractionation technique resulted in minimal cross contamination between the fractionated cellular compartments.

The placental lipid phenotype is associated with loss of methylation at the MEST DMD

The lipid accumulation phenotype in DNMT1o-deficient placentas suggested that genomic imprinting might regulate placental lipid metabolism. Therefore, we quantified methylation at 11 DMDs associated with placental function. DMD Methylation as a percent of WT methylation was determined and placentas were ranked by triacylglycerol concentration (Fig. 5A). Interestingly, of the 11 DMDs examined by univariate regression, only loss of methylation at the Mesoderm Specific Transcript (MEST) DMD was associated with accumulation of placental triacylglycerols (Fig. 5B). We have previously demonstrated, that as predicted, loss of methylation at the MEST DMD results in increased expression of *Mest* and decreased expression of *Klf14* (15). Methylation at the Peg10 DMD, while not reaching statistical significance ($p= 0.10$), was also negatively associated with placental triacylglycerol concentrations.

Discussion

Abnormal regulation of imprinted genes sheds light on the mechanisms by which genomic imprinting regulates placental processes to support fetal growth. Given the importance of fat to fetal growth, we focused our investigation on placental lipids and demonstrated that failure to maintain genomic imprinting resulted in the accumulation of triacylglycerols. We also found a novel association between disrupted genomic imprinting and altered mitochondrial function with impaired beta-oxidation and abnormal citrate metabolism. We hypothesize that mitochondrial oxidative stress contributed to abnormal citrate metabolism leading to lipid accumulation in DNMT1o-deficient placentas. Citrate is a key player that connects the metabolic pathways of the citric acid cycle in the mitochondria to fatty acid synthesis in the cytosol (26). Mitochondrial oxidative stress can increase *de novo* lipid synthesis as the iron-sulfur cluster of mitochondrial aconitase is inactivated by the generation of free radicals (27-29). Inhibition of mitochondrial aconitase leads to accumulation of citrate.

One possible interpretation of these data is that genomic imprinting evolved in part to regulate mitochondrial function and cellular metabolism to ensure normal fetal growth. Among DNMT1o-deficient embryos there is a strong inverse relationship between placental triglycerides and fetal growth. This is consistent with our understanding that mitochondrial dysfunction and oxidative stress is harmful to fetal growth (30). A link between genomic

imprinting and placental mitochondrial function is novel. To date, investigations of imprinted genes have focused on their regulation of discrete nutrient transporters in the placenta. Mitochondria regulate diverse cellular metabolic pathways-- catabolism of lipids, sugars, and amino acid metabolism, as well as critical steps in steroid hormone production. This positions them in a powerful place to influence fetal growth. It is unlikely that imprinted genes impair mitochondria directly as imprinted genes do not code for known mitochondrial proteins. Rather we suggest that dysregulation of imprinted genes could result in disruption of cellular metabolism that ultimately impairs mitochondrial function and fetal growth.

Previous studies have implicated mitochondrial dysfunction in mouse models of imprinted disorders, including the Prader-Willi and Angelman syndromes. A mouse model of Prader-Willi syndrome resulted in abnormal mitochondrial morphology, an increase in the activity of complex II and III in cardiac tissue, and altered expression of the genes regulating mitochondrial energetics (31). Likewise, a mouse model of Angelman syndrome showed abnormal mitochondrial morphology in the hippocampus and reduced complex III activity in the brain (32). Our methylation data implicate the MEST DMD in the DNMT1o placental lipid phenotype. The MEST DMD contains a number of genes that are definitively imprinted, including *Mest, Klf14, Cit1, and Cpa4* (33). Both *Mest* and *Klf14* have been linked to lipid biology, however, roles in mitochondrial biology are uncertain (34-36). *Mest* is predicted to act as a lipase from sequence homology with members of the alpha/beta fold hydrolase superfamily. Increased expression of *Mest* could lead to excess lipase activity and lipid accumulation. The accumulation of lipid droplets in non adipose tissue can result in lipotoxicity with resultant mitochondrial oxidative stress and further increased *de novo* lipid synthesis.

An alternative explanation for our data is that lipid accumulation and mitochondrial dysfunction are secondary to other processes induced by a generalized defect in genomic imprinting. For example, the abnormal trilaminar structure could cause localized trophoblast hypoxia, leading to oxidative damage and increased lipids (15). Analysis of our microarray data from DNMT1o-deficient placentas, did not demonstrate changes in expression of hypoxia inducible genes such as *Ndrg1, Dao2, Vegf, Pig7, Timp-3, Crf, or Gsta4* (37). This argues against the presence of significant hypoxia in these placentas.

Finally, our data highlight that fetal triacylglycerol concentrations are distinct from placental concentrations. The fetus may buffer excess lipids or convert placental lipids to other fuel sources such as carbohydrates. Lipotoxicity, however, may be the price the placenta pays for regulating delivery of lipids to the fetus. Thus, the excess lipid in DNMT1o-deficient placentas may contribute to placental dysfunction and substandard fetal growth via cellular toxicity rather than fetal fuel deprivation.

The findings presented here must be viewed in the context of several limitations. DNMT1o-deficiency results in epigenetic mosaics, due to stochastic loss of methylation and subsequent segregation of homologous chromosomes (4). This variation makes it difficult to dissect fine regulatory pathways. Furthermore, DNMT1o deficiency leads to a marked reduction in litter size, which could alter substrate availability to surviving embryos.

Additionally, given the effect on multiple DMDs it is challenging to determine what effects are primarily due to a defect in genomic imprinting and which effects are secondary. Finally, while we did not find important changes in the transcription of genes implicated in triacylglycerol trafficking, we did not assess protein concentrations or post-translational protein modifications. Despite these limitations, the lack of DNMT1o allows a comprehensive assessment of how genomic imprinting contributes to important placental processes.

Supplementary Material

Refer to Web version on PubMed Central for supplementary material.

Acknowledgments

We thank Nicole Kotchey for her assistance with cellular fractionation and Dr. Ben Van Houten, PhD for his assistance with mitochondrial studies. This work is supported by the Reproductive Scientist Development Program grant NIH K12 HD000849 (K.P.H) and National Institutes of Health Grants K12HD063087 (K.P.H) and NIH grant P01-HD069316 (to Y.S., Y.B, and J.R.C.) Use of the ultracentrifuge, as described, was made possible by NIH Grants UL1-RR024153 and UL1-TR000005.

References

1. Reinhart B, Eljanne M, Chaillet JR. Shared role for differentially methylated domains of imprinted genes. Molecular and cellular biology. 2002; 22(7):2089–98. [PubMed: 11884597]
2. Cirio MC, Ratnam S, Ding F, Reinhart B, Navara C, Chaillet JR. Preimplantation expression of the somatic form of Dnmt1 suggests a role in the inheritance of genomic imprints. BMC developmental biology. 2008; 8:9. [PubMed: 18221528]
3. Hirasawa R, Chiba H, Kaneda M, Tajima S, Li E, Jaenisch R, et al. Maternal and zygotic Dnmt1 are necessary and sufficient for the maintenance of DNA methylation imprints during preimplantation development. Genes & development. 2008; 22(12):1607–16. [PubMed: 18559477]
4. Cirio MC, Martel J, Mann M, Toppings M, Bartolomei M, Trasler J, et al. DNA methyltransferase 1o functions during preimplantation development to preclude a profound level of epigenetic variation. Developmental biology. 2008; 324(1):139–50. [PubMed: 18845137]
5. Doherty AS, Bartolomei MS, Schultz RM. Regulation of stage-specific nuclear translocation of Dnmt1o during preimplantation mouse development. Developmental biology. 2002; 242(2):255–66. [PubMed: 11820819]
6. Howell CY, Bestor TH, Ding F, Latham KE, Mertineit C, Trasler JM, et al. Genomic imprinting disrupted by a maternal effect mutation in the Dnmt1 gene. Cell. 2001; 104(6):829–38. [PubMed: 11290321]
7. Frost JM, Moore GE. The importance of imprinting in the human placenta. PLoS genetics. 2010; 6(7):e1001015. [PubMed: 20617174]
8. Sibley CP, Coan PM, Ferguson-Smith AC, Dean W, Hughes J, Smith P, et al. Placental-specific insulin-like growth factor 2 (Igf2) regulates the diffusional exchange characteristics of the mouse placenta. Proceedings of the National Academy of Sciences of the United States of America. 2004; 101(21):8204–8. [PubMed: 15150410]
9. Constancia M, Angiolini E, Sandovici I, Smith P, Smith R, Kelsey G, et al. Adaptation of nutrient supply to fetal demand in the mouse involves interaction between the Igf2 gene and placental transporter systems. Proceedings of the National Academy of Sciences of the United States of America. 2005; 102(52):19219–24. [PubMed: 16365304]
10. Tunster SJ, Tycko B, John RM. The imprinted Phlda2 gene regulates extraembryonic energy stores. Molecular and cellular biology. 2010; 30(1):295–306. [PubMed: 19884348]
11. Larque E, Ruiz-Palacios M, Koletzko B. Placental regulation of fetal nutrient supply. Current opinion in clinical nutrition and metabolic care. 2013; 16(3):292–7. [PubMed: 23416721]

12. Enzi G, Zanardo V, Caretta F, Inelmen EM, Rubaltelli F. Intrauterine growth and adipose tissue development. The American journal of clinical nutrition. 1981; 34(9):1785–90. [PubMed: 7282605]
13. Ghio A, Bertolotto A, Resi V, Volpe L, Di Cianni G. Triglyceride metabolism in pregnancy. Advances in clinical chemistry. 2011; 55:133–53. [PubMed: 22126027]
14. Woollett LA. Review: Transport of maternal cholesterol to the fetal circulation. Placenta. 2011; 32(Suppl 2):S218–21. [PubMed: 21300403]
15. Himes KP, Koppes E, Chaillet JR. Generalized disruption of inherited genomic imprints leads to wide-ranging placental defects and dysregulated fetal growth. Developmental biology. 2013; 373(1):72–82. [PubMed: 23085235]
16. Ehrich M, Nelson MR, Stanssens P, Zabeau M, Liloglou T, Xinarianos G, et al. Quantitative high-throughput analysis of DNA methylation patterns by base-specific cleavage and mass spectrometry. Proceedings of the National Academy of Sciences of the United States of America. 2005; 102(44):15785–90. [PubMed: 16243968]
17. Peters J. The role of genomic imprinting in biology and disease: an expanding view. Nature reviews Genetics. 2014; 15(8):517–30.
18. Livak KJ, Schmittgen TD. Analysis of relative gene expression data using real-time quantitative PCR and the 2(-Delta Delta C(T)) Method. Methods. 2001; 25(4):402–8. [PubMed: 11846609]
19. Lawton KA, Berger A, Mitchell M, Milgram KE, Evans AM, Guo L, et al. Analysis of the adult human plasma metabolome. Pharmacogenomics. 2008; 9(4):383–97. [PubMed: 18384253]
20. Sreekumar A, Poisson LM, Rajendiran TM, Khan AP, Cao Q, Yu J, et al. Metabolomic profiles delineate potential role for sarcosine in prostate cancer progression. Nature. 2009; 457(7231):910–4. [PubMed: 19212411]
21. Folch J, Lees M, Sloane Stanley GH. A simple method for the isolation and purification of total lipides from animal tissues. The Journal of biological chemistry. 1957; 226(1):497–509. [PubMed: 13428781]
22. Mo FE, Muntean AG, Chen CC, Stolz DB, Watkins SC, Lau LF. CYR61 (CCN1) is essential for placental development and vascular integrity. Molecular and cellular biology. 2002; 22(24):8709–20. [PubMed: 12446788]
23. Gasnier F, Rousson R, Lerme F, Vaganay E, Louisot P, Gateau-Roesch O. Use of Percoll gradients for isolation of human placenta mitochondria suitable for investigating outer membrane proteins. Analytical biochemistry. 1993; 212(1):173–8. [PubMed: 8396360]
24. Ducharme NA, Bickel PE. Lipid droplets in lipogenesis and lipolysis. Endocrinology. 2008; 149(3):942–9. [PubMed: 18202123]
25. Farese RV Jr, Walther TC. Lipid droplets finally get a little R-E-S-P-E-C-T. Cell. 2009; 139(5): 855–60. [PubMed: 19945371]
26. Lanaspa MA, Sanchez-Lozada LG, Choi YJ, Cicerchi C, Kanbay M, Roncal-Jimenez CA, et al. Uric acid induces hepatic steatosis by generation of mitochondrial oxidative stress: potential role in fructose-dependent and -independent fatty liver. The Journal of biological chemistry. 2012; 287(48):40732–44. [PubMed: 23035112]
27. Hausladen A, Fridovich I. Superoxide and peroxynitrite inactivate aconitases, but nitric oxide does not. The Journal of biological chemistry. 1994; 269(47):29405–8. [PubMed: 7961919]
28. Gardner PR. Superoxide-driven aconitase FE-S center cycling. Bioscience reports. 1997; 17(1):33–42. [PubMed: 9171919]
29. Scandroglio F, Tortora V, Radi R, Castro L. Metabolic control analysis of mitochondrial aconitase: influence over respiration and mitochondrial superoxide and hydrogen peroxide production. Free radical research. 2014; 48(6):684–93. [PubMed: 24601712]
30. Burton GJ, Yung HW, Cindrova-Davies T, Charnock-Jones DS. Placental endoplasmic reticulum stress and oxidative stress in the pathophysiology of unexplained intrauterine growth restriction and early onset preeclampsia. Placenta. 2009; 30(Suppl A):S43–8. [PubMed: 19081132]
31. Yazdi PG, Su H, Ghimbovschi S, Fan W, Coskun PE, Nalbandian A, et al. Differential gene expression reveals mitochondrial dysfunction in an imprinting center deletion mouse model of Prader-Willi syndrome. Clinical and translational science. 2013; 6(5):347–55. [PubMed: 24127921]

32. Su H, Fan W, Coskun PE, Vesa J, Gold JA, Jiang YH, et al. Mitochondrial dysfunction in CA1 hippocampal neurons of the UBE3A deficient mouse model for Angelman syndrome. Neuroscience letters. 2011; 487(2):129–33. [PubMed: 19563863]

33. Yamada T, Mitsuya K, Kayashima T, Yamasaki K, Ohta T, Yoshiura K, et al. Imprinting analysis of 10 genes and/or transcripts in a 1.5-Mb MEST-flanking region at human chromosome 7q32. Genomics. 2004; 83(3):402–12. [PubMed: 14962666]

34. Nikonova L, Koza RA, Mendoza T, Chao PM, Curley JP, Kozak LP. Mesoderm-specific transcript is associated with fat mass expansion in response to a positive energy balance. FASEB journal: official publication of the Federation of American Societies for Experimental Biology. 2008; 22(11):3925–37. [PubMed: 18644838]

35. Frank D, Fortino W, Clark L, Musalo R, Wang W, Saxena A, et al. Placental overgrowth in mice lacking the imprinted gene Ipl. Proceedings of the National Academy of Sciences of the United States of America. 2002; 99(11):7490–5. [PubMed: 12032310]

36. Lin SP, Youngson N, Takada S, Seitz H, Reik W, Paulsen M, et al. Asymmetric regulation of imprinting on the maternal and paternal chromosomes at the Dlk1-Gtl2 imprinted cluster on mouse chromosome 12. Nature genetics. 2003; 35(1):97–102. [PubMed: 12937418]

37. Roh CR, Budhraja V, Kim HS, Nelson DM, Sadovsky Y. Microarray-based identification of differentially expressed genes in hypoxic term human trophoblasts and in placental villi of pregnancies with growth restricted fetuses. Placenta. 2005; 26(4):319–28. [PubMed: 15823618]

Highlights

- The role genomic imprinting plays in regulating placental lipids is unknown.
- A global disruption of imprints results in accumulation of placental triacylglycerols.
- Disruption of imprints leads to abnormal citrate metabolism.
- Loss of methylation at the MEST DMD is associated with triacylglycerol accumulation.

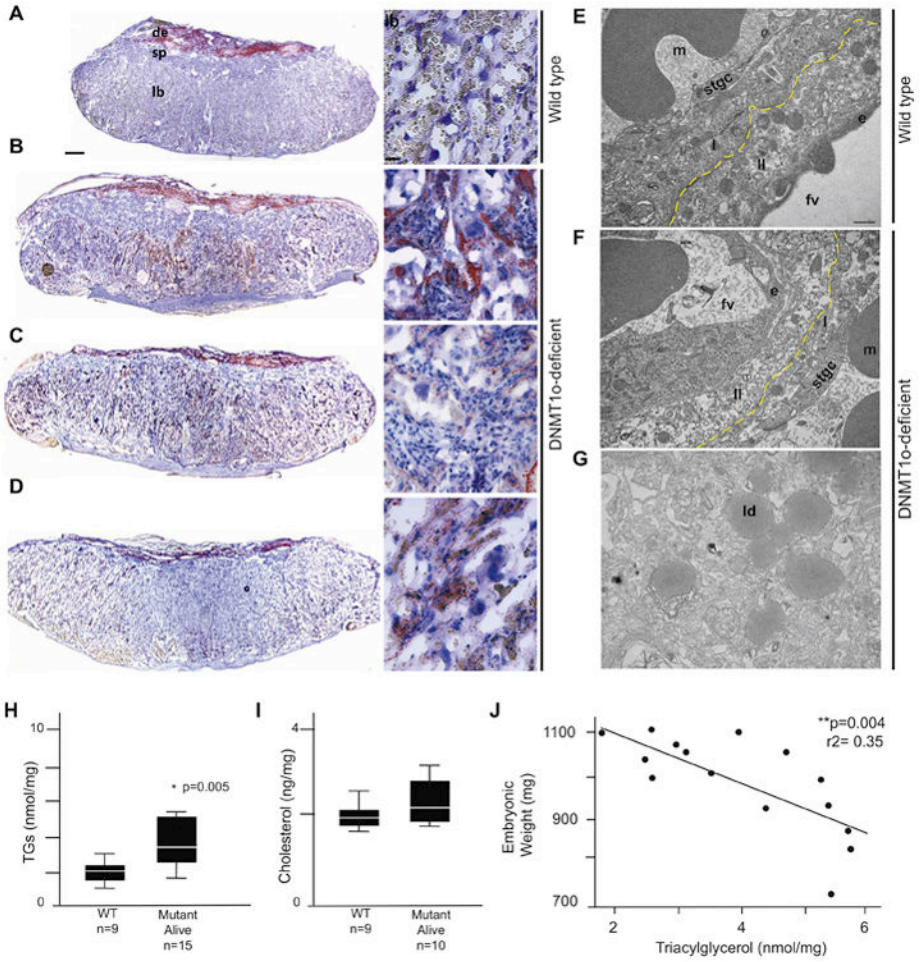

Fig. 1. A generalized disruption in genomic imprinting leads to accumulation of triacylglycerols in the placenta at E17.5

(A-D) Staining with oil red O in representative wild type (A) and DNMT1o-deficient placentas (B-D). Maternal decidua serves as a positive control. (E-G) Electron micrographs of labyrinth of E17.5 wild type (E) and DNMT1o-deficient placentas (F,G). Yellow dotted line indicates the junction between trophoblast layers I and II. (H,I) Box plots showing median values, upper and lower quartiles, and range of triacylglycerol and cholesterol among wild type and DNMT1o-deficient placentas. (J) Relationship between embryonic weight and placental triacylglycerols among mutants. TGs=Triacylglycerols. WT=Wild type. de=Decidua. sp=Spongiotrophoblast. lb=Labyrinth. fv= fetal vessel, e= endothelium. stgc= sinusoidal trophoblast giant cells. m= maternal. ld= lipid droplet. Scale bar (A-D) 400 μm (left panel) and 100 μm (right panel). Scale bar (E-G) 2 μm (left panel) and 500 nm (right panel).* Denotes significant difference compared to wild type by Kruskal-Wallis.** Analysis by linear regression.

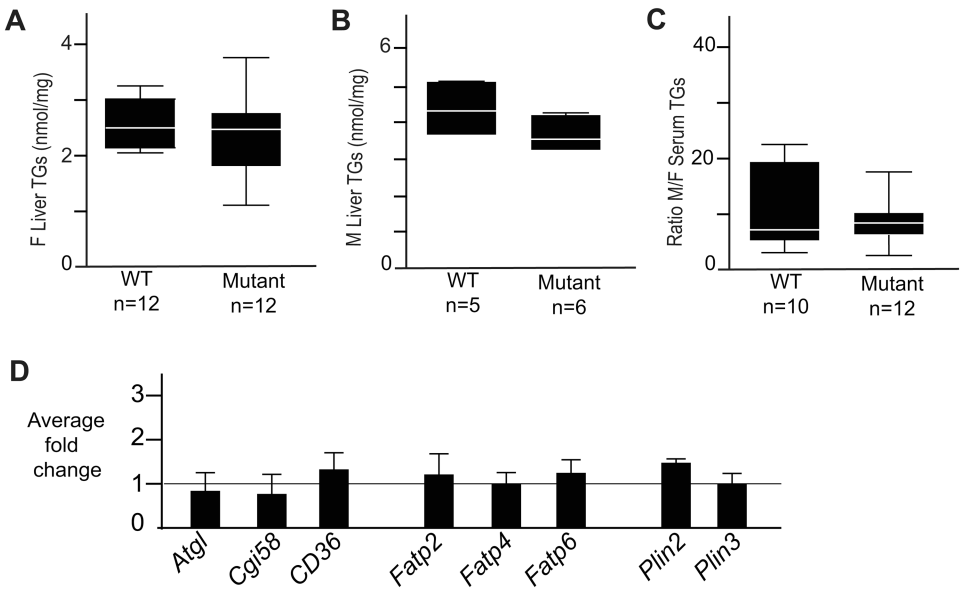

Fig. 2. Maternal and fetal triacylglycerols are not altered by DNMT1o deficiency

Placental triacylglycerols, however, are inversely associated with embryonic weight among mutants. (A-C) Box plots showing median values, upper and lower quartiles and range of fetal and maternal triacylglycerol in liver, and ratio of maternal/fetal serum among wild type and DNMT1o-deficient animals. Ratios are derived from 3 WT dams and their 10 WT embryos and 5 DNMT1o-deficient dams and their 12 DNMT10-deficient embryos. (D) Expression of genes critical for lipid trafficking. The histogram summarizes mean expression (+SEM) of genes in DNMT1o-deficient placentas compared to wild type. n=15 DNMT1o-deficient placentas; n=10 wild type. F=Fetal. M=Maternal. TGs=Triacylglycerols. WT=Wild type.

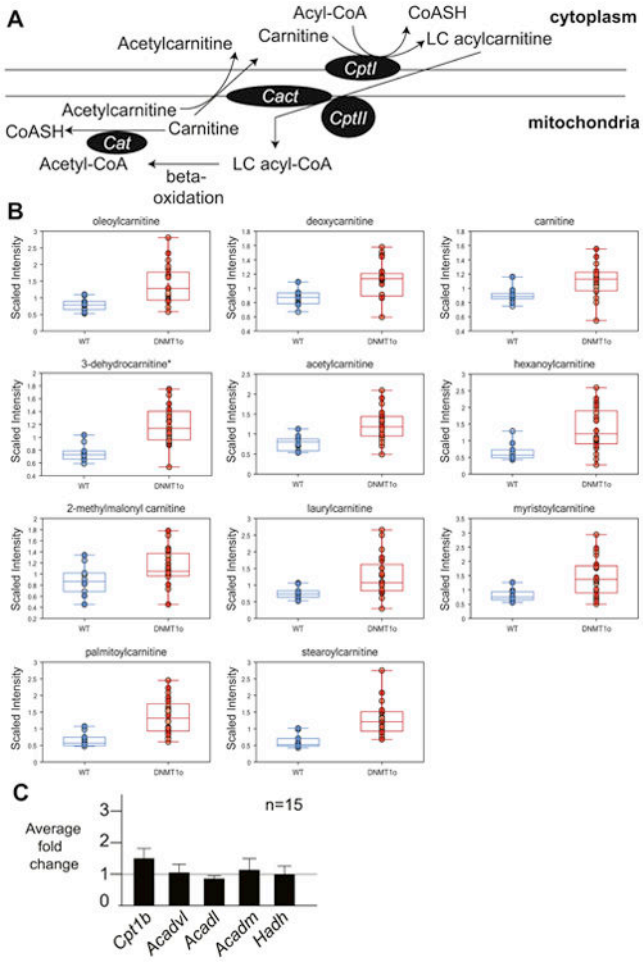

Fig. 3. DNMT1o-deficient placentas accumulate acylcarnitines of various chain lengths, suggesting altered fatty acid oxidation

(A) Schematic outlining critical components of fatty acid oxidation. Carnitine shuttles long-chain fatty acids across the mitochondrial membrane for fatty acid oxidation. (B) Box plots of various acylcarnitines measured as part of a global biochemical profile of wild type and DNMT1o-deficient placentas. Following log transformation, ANOVA was used to identify biochemicals that differed significantly between wild type and DNMT1o-deficient placentas. All box plots presented have $p<0.05$ by ANOVA. n=10 wild type and n=20 DNMT1o-deficient placentas. (C) Expression of genes involved in fatty acid oxidation in the placenta among DNMT1o-deficient placentas compared to wild type. The histogram summarizes mean expression (+SEM) of genes in DNMT1o-deficient placentas compared to wild type.

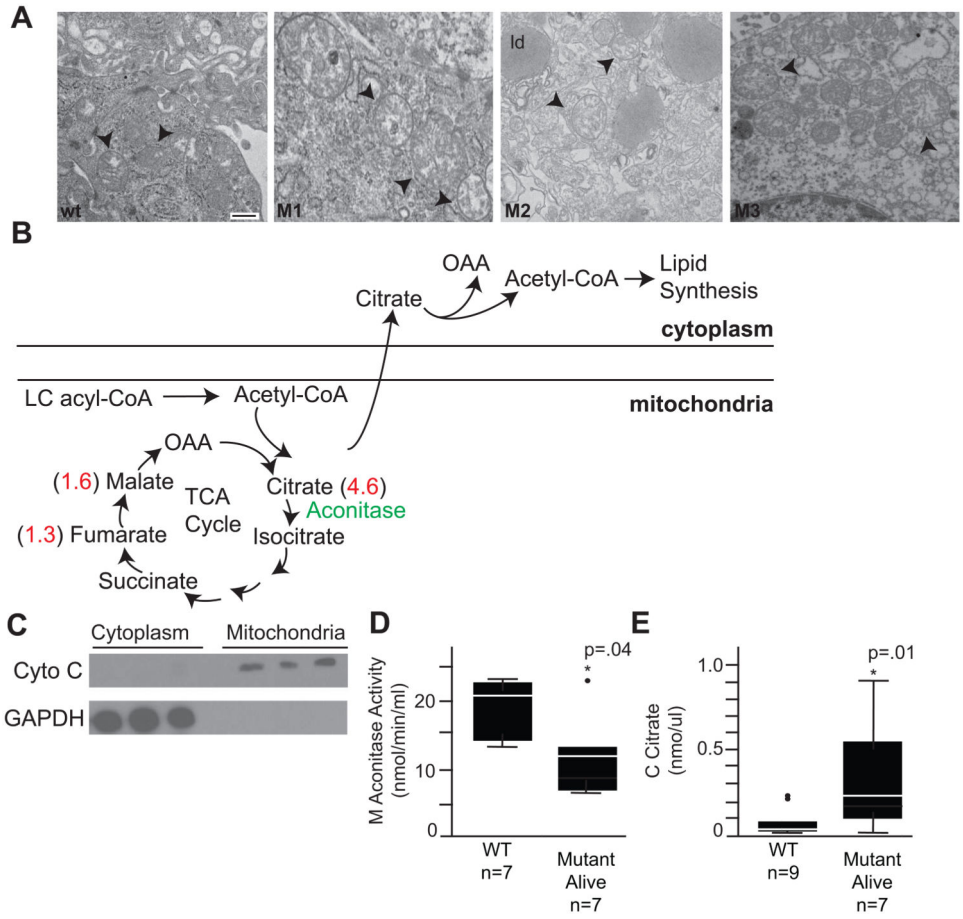

Fig. 4. A generalized disruption of genomic imprints induces changes in mitochondrial morphology and mitochondrial oxidative stress

(A) Transmission electron microscopy of wild type and DNMT1o-deficient placentas demonstrates abnormal mitochondria in mutant placentas. Mitochondria are marked with arrowheads. (B) Schematic highlighting the central role that citrate plays in *de novo* lipid synthesis. Metabolomics profiling of biochemicals involved in the TCA cycle are highlighted in red. (C) Western blot of representative wild type and DNMT1o-deficient cytoplasmic and mitochondrial fractions obtained from placenta. Cytochrome c was used as a marker of mitochondria and GAPDH as a marker of cytoplasm. (D,E) Box plots showing median values, upper and lower quartiles, and range of mitochondrial aconitase activity (D) and cytoplasmic citrate concentrations (E). WT=wild type. M1-M3=DNMT1o-deficient placentas 1-3. ld=lipid droplet. Scale bar=500nm. M=mitochondria. C=Cytoplasm. * Analysis by Kruskal-Wallis.

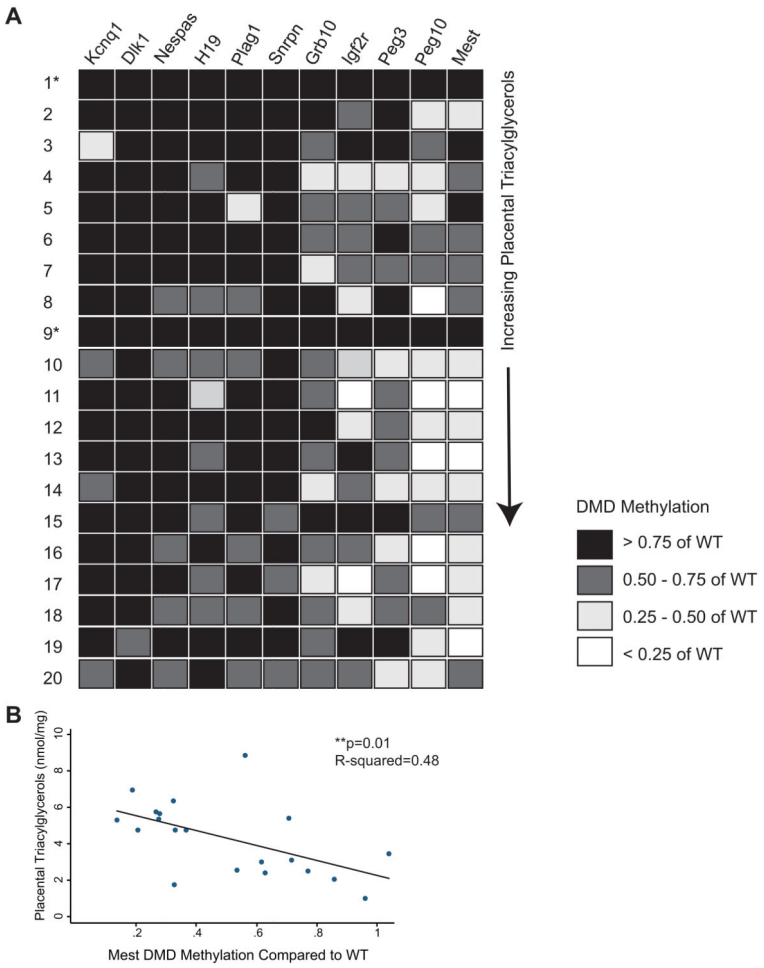

Fig. 5. Loss of methylation at the MEST DMD is strongly associated with placental triacylglycerol concentrations

(A) Methylation analysis at 11 imprinted DMDs in 20 placentas was done using EpiTyper analysis. DMD methylation was compared to wild type and then ranked by increasing concentration of triacylglycerols in the placenta. (B) Loss of methylation at MEST is inversely associated with placental triacylglycerol concentrations. wt=wild type. DMD=differentially methylated domain. * Indicate wt placentas. ** Analysis by linear regression.

Table 1

Lipid pathways assessed in DNMT1o-deficient placentas compared to wild type (mt/wt)

Lipid Sub Pathway	Biochemicals with p≤0.05/ biochemicals assayed for pathway	Biochemicals ⇑|⇓
Essential fatty acids	1/7	1|0
Medium chain fatty acids	1/2	1|0
Long chain fatty acids	2/23	2|0
Fatty acid, monohydroxy	2/4	2|0
Fatty acid, branched	0/2	
Eicosanoid	3/4	0|3
Endocannabinoid	0/3	
Fatty acid metabolism	2/3	2|0
Carnitine metabolism	10/11	10|0

Lipid Sub Pathway	**Biochemicals with p≤0.05/ biochemicals assayed for pathway**	Biochemicals ⇑|⇓
Bile acid metabolism	2/4	
Glycerolipid metabolism	3/5	
Inositol metabolism	2/5	
Ketone bodies	0/1	
Lysolipid	5/12	
Monoacylglycerol	1/4	
Diacylglycerol	0/2	
Sphingolipid	3/5	
Sterol/Steroid	2/6